Supporting Information

Photocatalytic oxidation of glycerol with red light employing quinacridone sensitized TiO_2 nanoparticles

Yunshuo Yang,[a] Marco Nalesso,[a] Andrea Basagni,[a] Ruggero Bonetto,[a] Raffaella Signorini,[a] Stefano Agnoli,[a] Luka Đorđević, [a],* Andrea Sartorel [a],*

[a] Department of Chemical Sciences, University of Padova, via Marzolo 1, 35131 Padova, Italy. E-mail addresses: luka.dordevic@unipd.it; andrea.sartorel@unipd.it

Index

Irradiation sources in photocatalysis experiments[1,2]

Light driven experiments were conducted with home-made photoreactors and using different irradiation sources, with modulating power. The emission spectra of the light sources are shown in Figure S1.

Light type	Irradiation	Light source	Application
White light	33 $mWcm^{-2}$	Commercial white LED	TMB oxidation
White light	200 $mWcm^{-2}$	Godox-SL600IID lamp placed at 3.5 cm	Glycerol oxidation
Green Light	λ_{MAX} 525 nm FWHM 30 nm 7.9 $mWcm^{-2}$	Cree XLamp XP-E2 Color High Power LED Star From LED supply	AQY determination (TMB oxidation)
Green Light	λ_{MAX} 525 nm FWHM 30 nm 120 $mWcm^{-2}$	Cree XLamp XP-E2 Color High Power LED Star From LED supply	Glycerol oxidation
Yellow Light	λ_{MAX} 590 nm FWHM 15 nm 7.3 $mWcm^{-2}$	Cree XLamp XP-E2 Color High Power LED Star From LED supply	AQY determination (TMB oxidation)
Yellow Light	λ_{MAX} 590 nm FWHM 79 nm 200 $mWcm^{-2}$	Cree XLamp XP-E2 Color High Power LED Star From LED supply	Glycerol oxidation
Red Light	λ_{MAX} 620 nm FWHM 15 nm 19.3 $mWcm^{-2}$	Cree XLamp XP-E2 Color High Power LED Star From LED supply	AQY determination (TMB oxidation)
Red Light	λ_{MAX} 620 nm FWHM 15 nm 33 $mWcm^{-2}$	Cree XLamp XP-E2 Color High Power LED Star From LED supply	Glycerol oxidation
Red Light	λ_{MAX} 740 nm FWHM 37 nm 9.1 $mWcm^{-2}$	Cree XLamp XP-E2 Color High Power LED Star From LED supply	AQY determination (TMB oxidation)

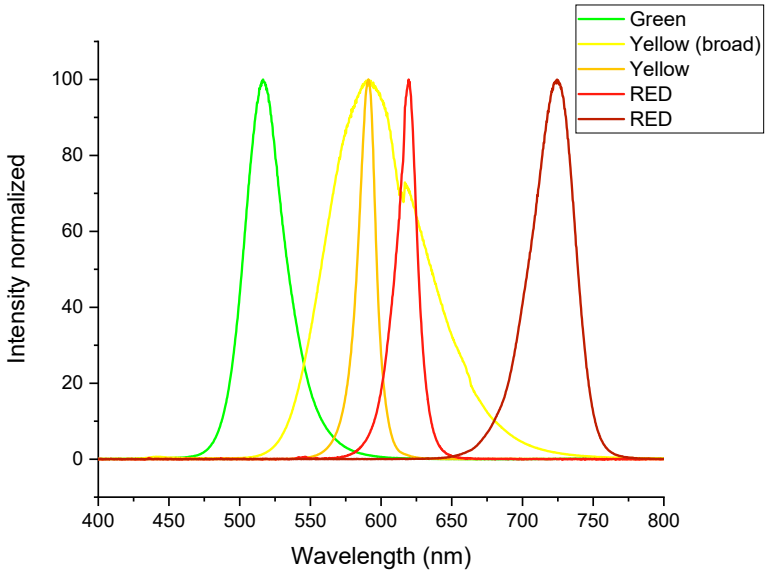

Figure S1. Emission spectra of the light sources employed in this work.

Products quantification was performed by high performance liquid chromatography (HPLC) using an Agilent Technologies 1260 Infinity II LC system coupled to diode array detector; the instrument is equipped with Hi-Plex H column 300×7.7 mm. Condition of analysis: [H_2SO_4] = 5 mM in milliQ water as eluent, isocratic gradient, flow rate 0.7 mL·min^{-1}, injected volume 20 µL, temperature 50 °C. Calibration curves were obtained for GLAD, DHA, GA, FA.

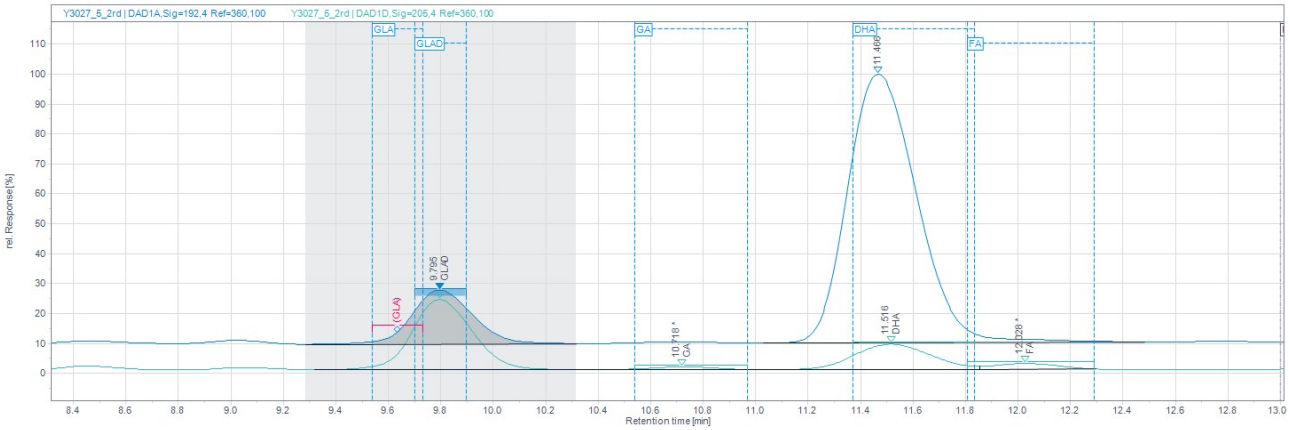

Figure S2. Representative chromatogram for the analysis of the reaction mixture.

Estimation of the average QA layer thickness with a spherical model on QA_L@TiO_2 nanoparticles

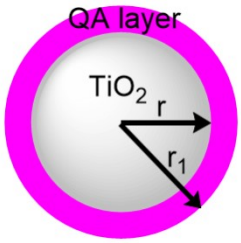

We estimated the average thickness of the QA film employing a spherical model of the QA_L@TiO_2 nanoparticles. Assuming a spherical shape of the TiO_2 particles with a diameter of 21 nm and radius r = 10.5 nm, this results in a volume of a TiO_2 nanoparticle of 4850 nm^3 and in a mass of $2.05 \cdot 10^{-17}$ g (given a density for TiO_2 of 4.23 gcm^{-3}). Taking QA_{312}@TiO_2 nanoparticles as a reference material, the w/w amount of QA in QA_{312}@TiO_2 is 10%, resulting in $2.3 \cdot 10^{-18}$ g of QA, that corresponds to a volume of 1550 nm^3 of the QA purple layer (given the density of QA of 1.47 gcm^{-3}). The total volume of a QA_{312}@TiO_2 nanoparticle is thus 6400 nm^3, from which a radius r_1 = 11.5 can be derived. The average QA layer is thus expected to be around r_1-r = 1 nm.

Material	QA:TiO_2 w/w %	QA layer average thickness / nm
QA_{16}@TiO_2	0.5	0.06[a]
QA_{78}@TiO_2	2.5	0.27
QA_{156}@TiO_2	5	0.53
QA_{312}@TiO_2	10	1
QA_{624}@TiO_2	20	1.9

[a]This low value may indicate an incomplete coverage of the TiO_2 surface.

Apparent Quantum Yield determination

The apparent quantum yield AQY for TMB oxidation was obtained with different lights. Conditions: 0.2 mM TMB with 1mg·mL^{-1} QA_{312}@TiO_2 nanoparticles in 2 mL of 0.1 M aqueous acetate buffer (pH 5) in 10 mins.

Table S1. Apparent Quantum Yield for TMB oxidation.

Light (photon flux / einstein $s^{-1}cm^{-2}$)	**Photons[a] / Einstein**	**Absorption@652nm**	**Molecules of TMB oxidized[b]**	**AQY**
525 nm, 7.9 mW cm^{-2} (2.08×10^{16})	2.29×10^{19}	0.032	9.88×10^{15}	0.043%
590 nm, 7.3 mW cm^{-2} (2.16×10^{16})	1.99×10^{19}	0.020	6.17×10^{15}	0.031%
620 nm, 19.3 mW cm^{-2} (6.01×10^{16})	6.58×10^{19}	0.035	1.09×10^{16}	0.016%
740 nm, 9.1 mW cm^{-2} (3.38×10^{16})	3.13×10^{20}	0	0	0%

[a] in 10 minutes of irradiation, considering the surface of the solution irradiated. [b] calculated using an ε = 3.9 10^4 $M^{-1}cm^{-1}$ for the charge transfer adduct.[3]

Supplementary Figures

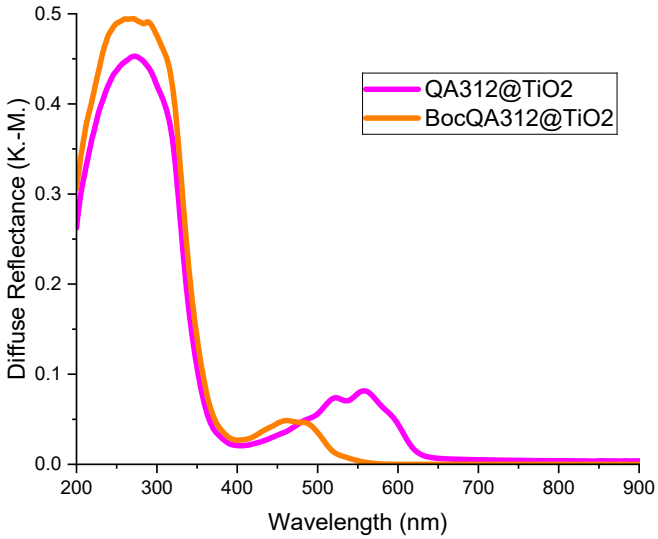

Figure S3. Diffuse Reflectance spectra reported in Kubelka-Munk units of Boc-QA_{312}@TiO_2 and of QA_{312}@TiO_2 (3% w/w in $BaSO_4$).

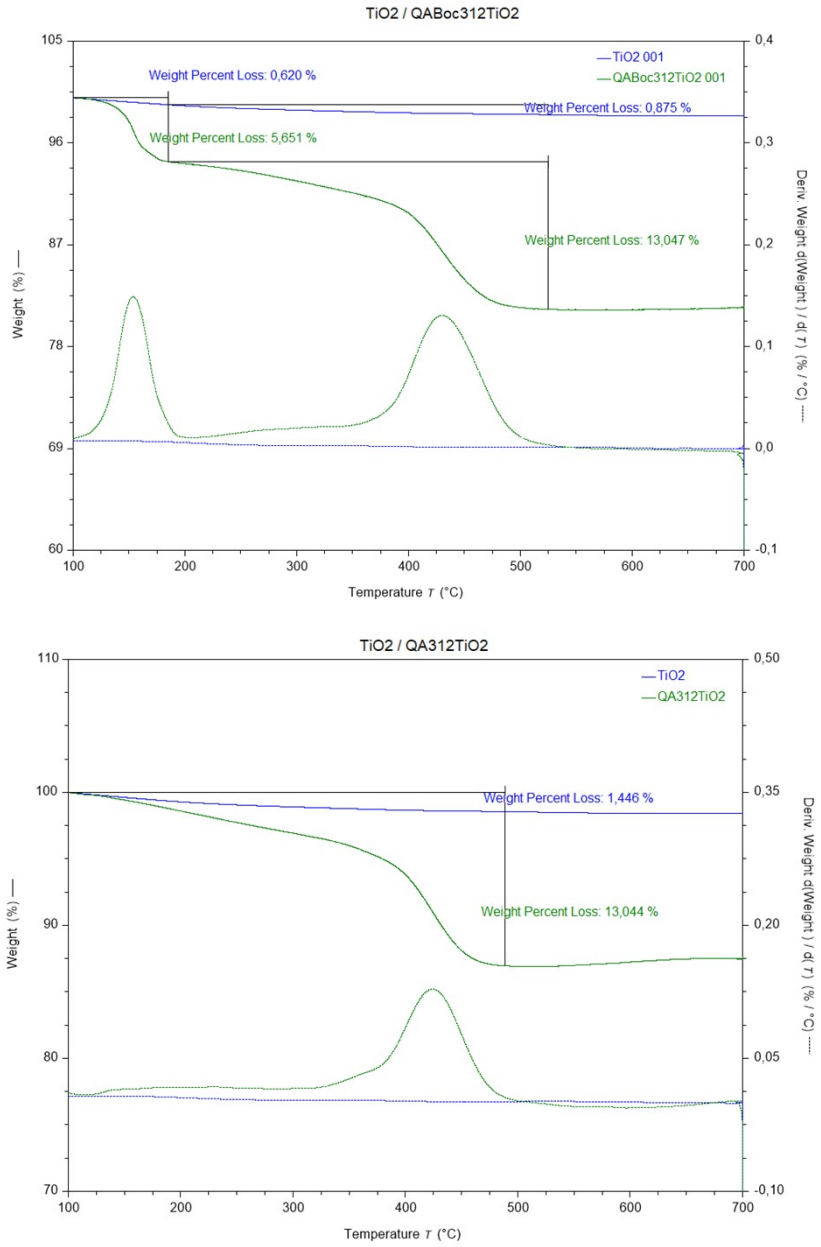

Figure S4. Thermogravimetric analysis of Boc-QA_{312}@TiO_2 (top panel) and of QA_{312}@TiO_2 (bottom panel). In every graph the TGA of TiO_2 nanoparticles is also shown in the blue trace as a comparison. In the case of QA_{312}@TiO_2, the weight loss of11.6% associated to the first derivative curve with maximum at 430 °C is attributed to QA loss, and shows a good consistency with the 9.6% w/w amount of QA from the nominal loading.

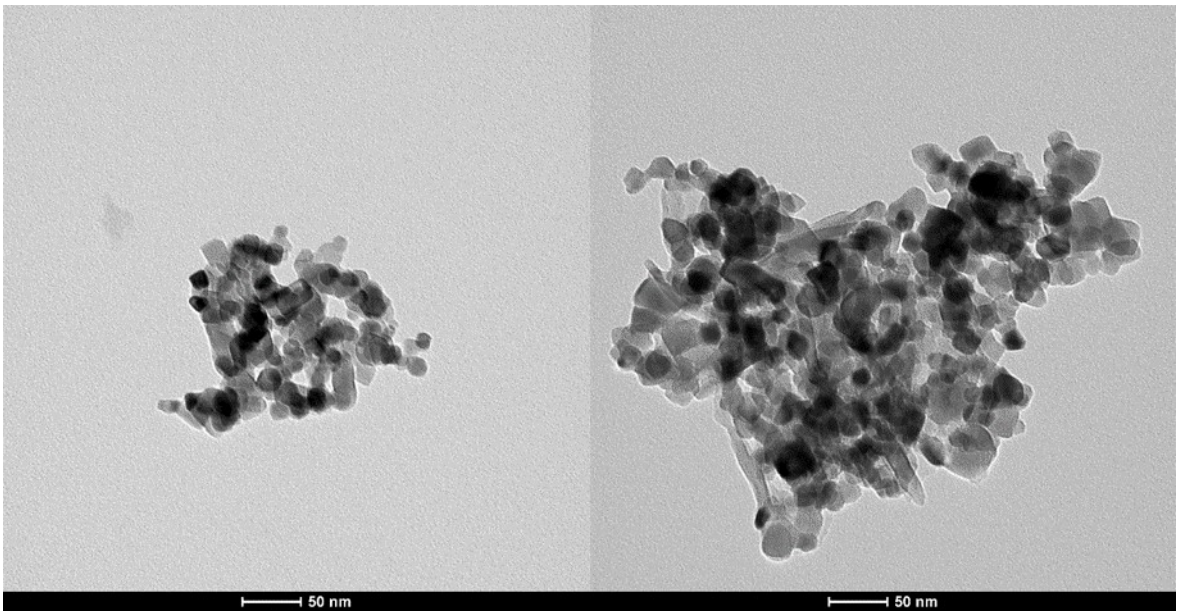

Figure S5. Transmission Electron Microscopy (TEM) images of TiO_2 nanoparticles (left) and of $QA_{312}@TiO_2$ nanoparticles (right).

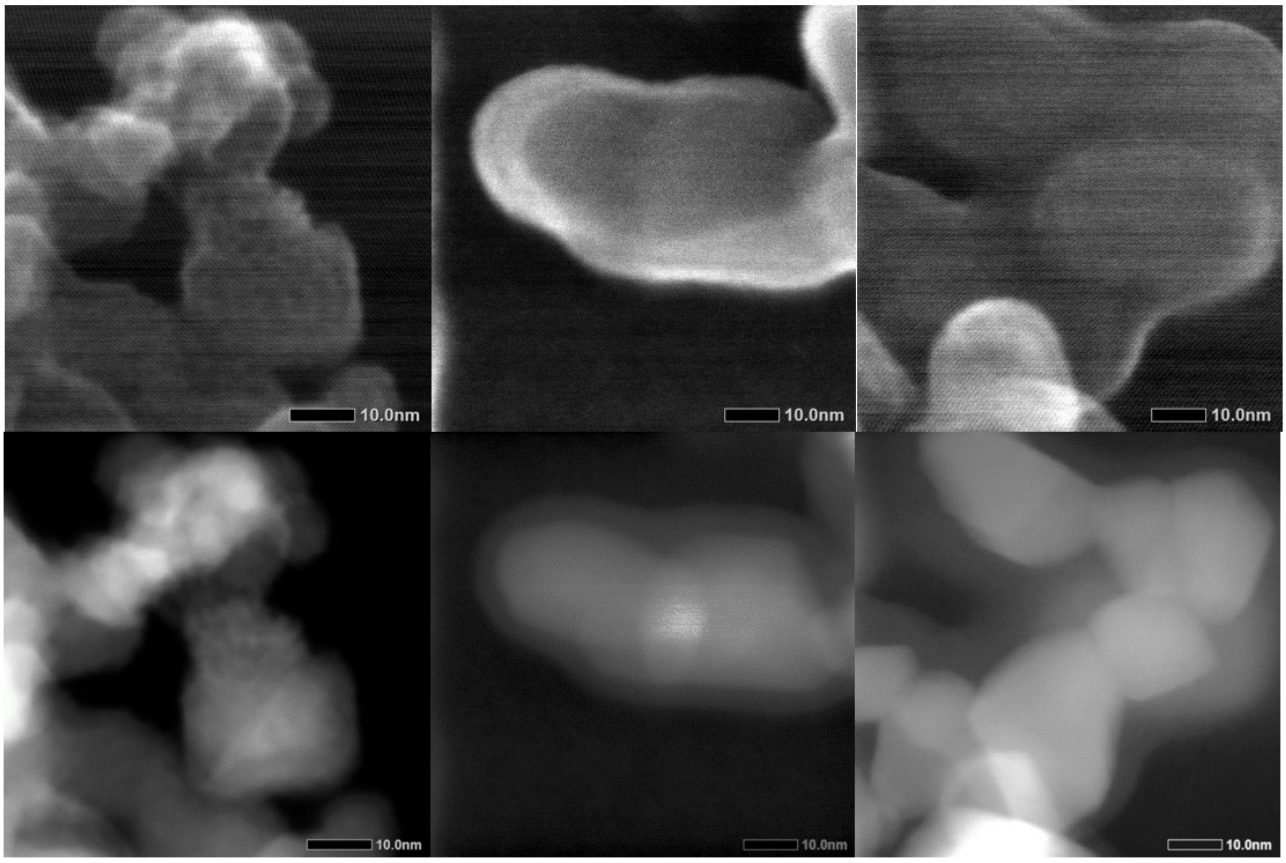

Figure S6. Scanning transmission electron microscopy (STEM) of TiO2 (left), $QA_{16}@TiO_2$ (middle), $QA_{312}@TiO_2$ (right). Bottom: HAADF-STEM images of the same materials.

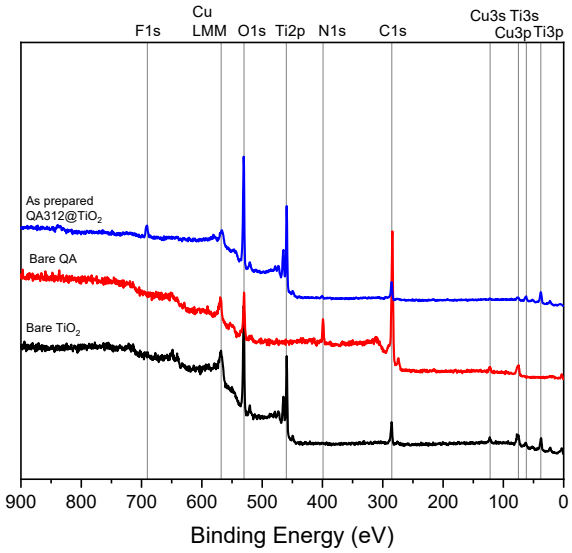

Figure S7. Survey XPS scan of $QA_{312}@TiO_2$, bare QA and bare TiO_2

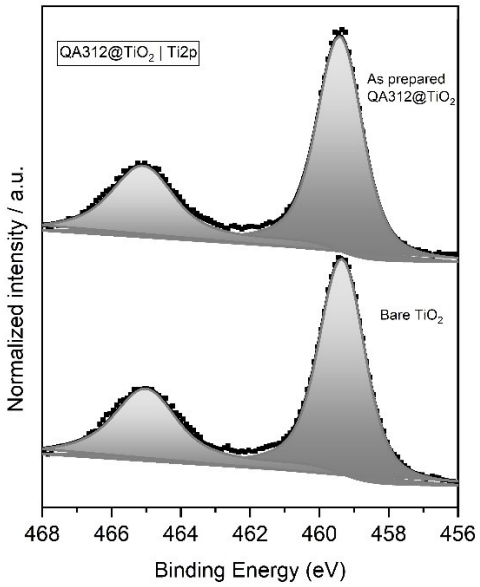

Figure S8. XPS (Ti 2*p* region) of $QA_{312}@TiO_2$ (top) and of TiO_2 (bottom).

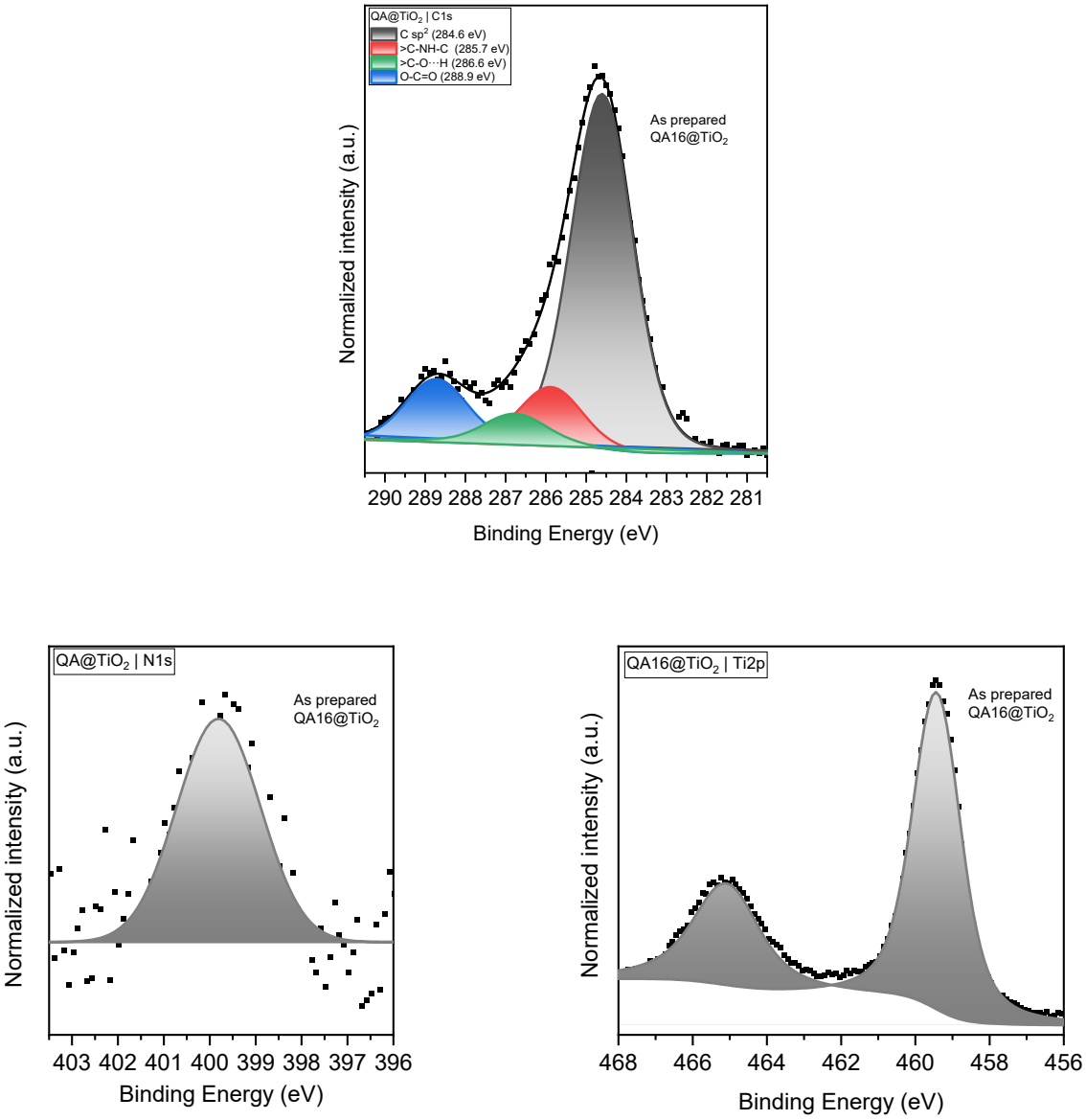

Figure S9. XPS analysis of $QA_{16}@TiO_2$ (C, N, Ti regions).

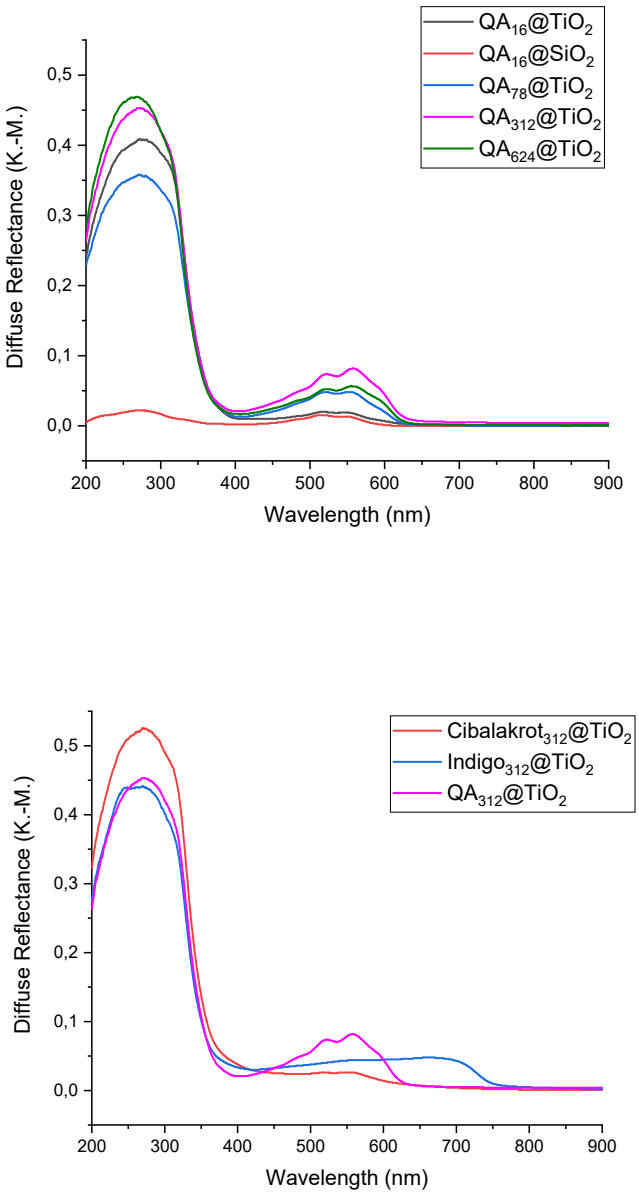

Figure S10. Top: diffuse reflectance spectra of $QA_L@TiO_2$ and $QA_{16}@SiO_2$ NPs. The spectra show an increase of the optical absorption in the visible region with increasing the amount of QA up to a loading of 624 μmol·gTiO_2. The intensity of the absorption is however not proportional to the QA loading, since the surface of the TiO_2 NPs is mostly covered with QA even at the lower loading. Bottom: diffuse reflectance spectra of $Indigo_{312}@TiO_2$ and $Cibalakrot_{312}@TiO_2$ NPs.

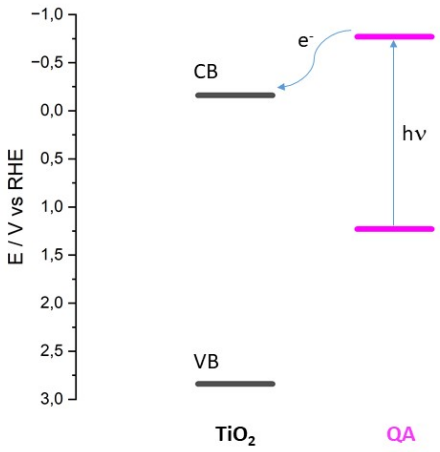

Figure S11. Energy levels of QA and TiO_2.

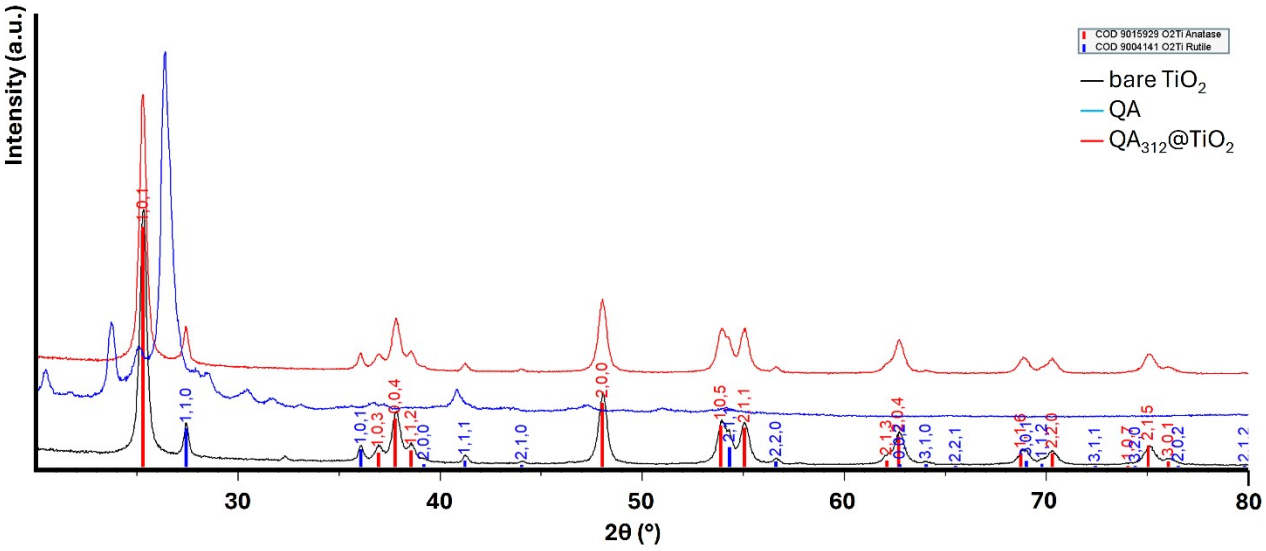

Figure S12. XRD patterns of bare TiO_2 (black line), QA (blue line) and $QA_{312}@TiO_2$ (red line). Sticks are superimposed at the bottom where the expected reflections lie for Anatase (COD9015929) and Rutile (COD9004141). In the commercial QA, the diffractogram is consistent with the γ-polymorph.[4]

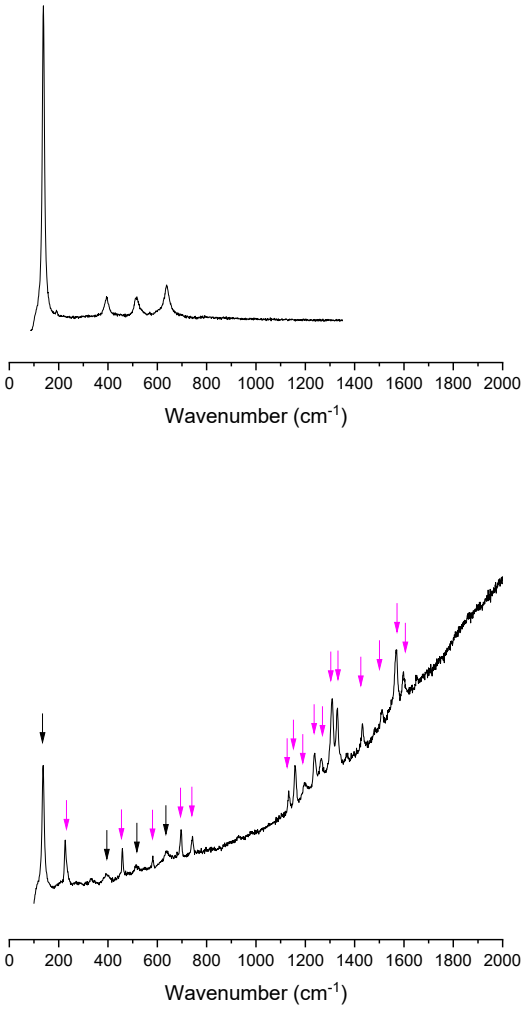

Figure S13. Resonant Raman experiments of TiO_2 (top) and of $QA_{312}@TiO_2$ NPs (bottom). TiO_2 NPs show Raman shifts at 138, 395, 514 and 637 cm^{-1} (black arrows); peaks attributable to the QA pigment (purple arrows) are observed at 226, 328, 458, 582, 693, 744, 1134, 1160, 1199, 1238, 1264, 1310, 1329, 1433, 1511, 1570, 1596 cm^{-1}. In the spectrum of $QA_{312}@TiO_2$ NPs, the raising of the baseline above 1000 cm^{-1} is due to fluorescence of the QA pigment. In the 100 – 300 cm^{-1} region, the peak at 138 cm^{-1} is due to TiO_2, the peak at 226 cm^{-1} is attributed to the QA γ polymorph.

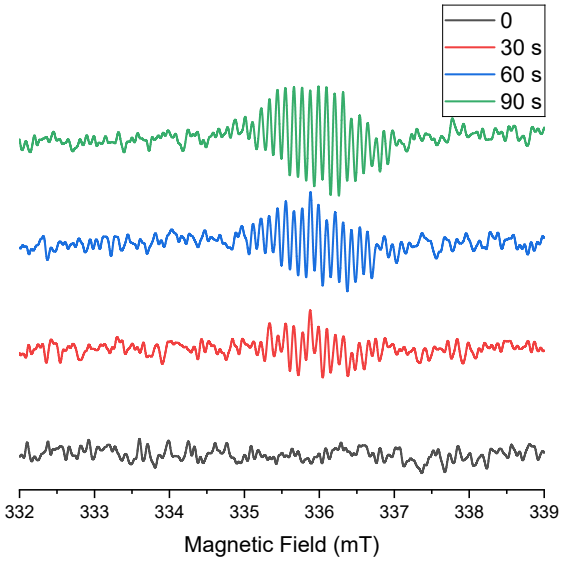

Figure S14. EPR analysis recorded at different irradiation time in the photochemical oxidation of TMB. The spectrum is attributable to $TMB^{\cdot+}$.[3]

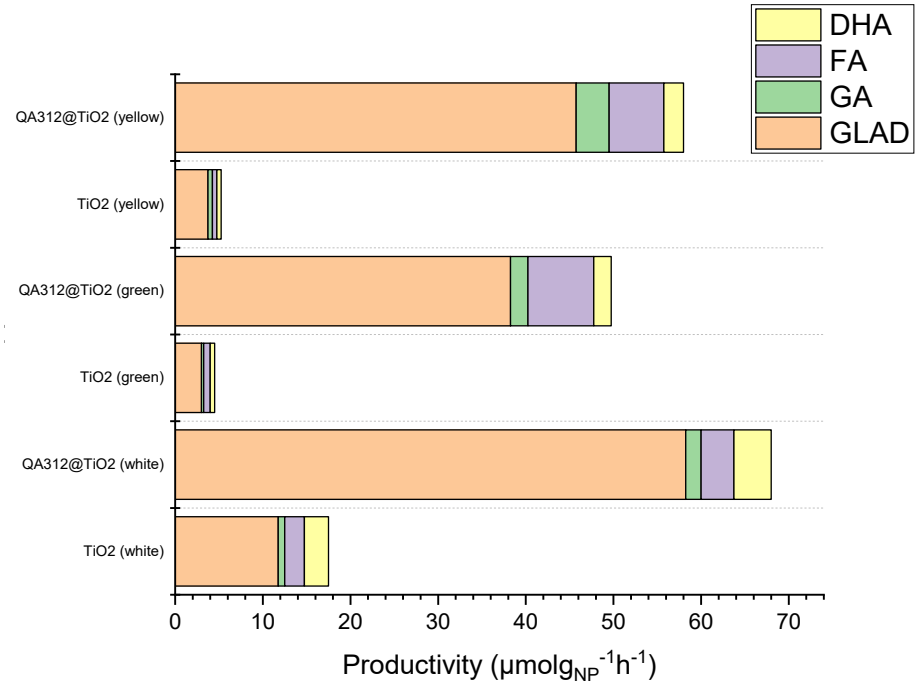

Figure S15. Glycerol oxidation with TiO_2 and $QA_{312}@TiO_2$ nanoparticles employing yellow, green and white light.

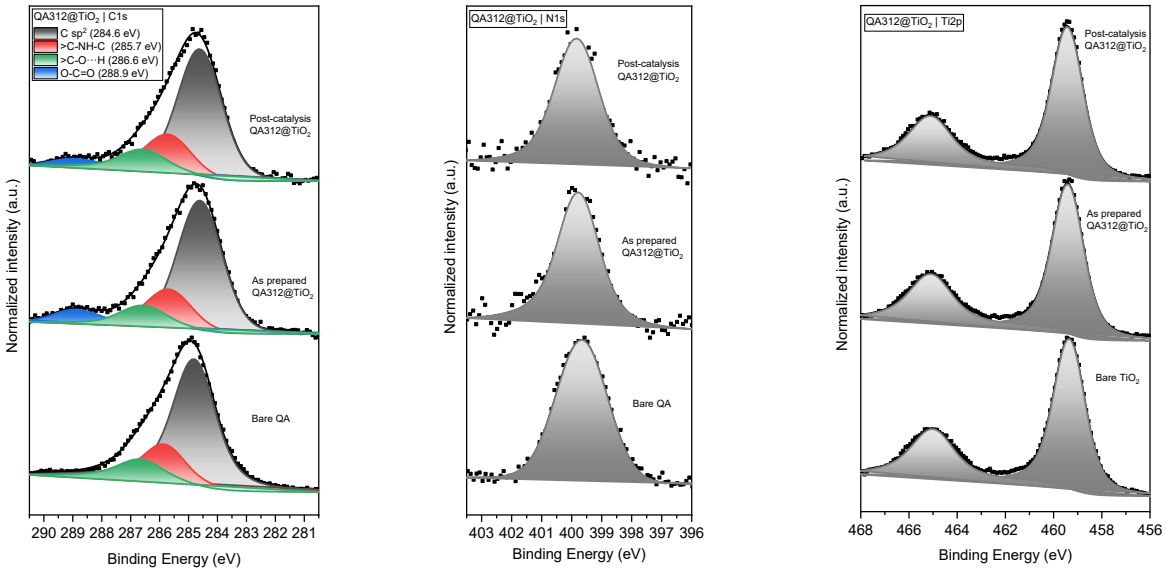

Figure S16. XPS of $QA_{312}@TiO_2$ nanoparticles post catalysis compared to as prepared $QA_{312}@TiO_2$ and QA.

Supplementary Tables

Table S2. Literature systems for photochemical glycerol oxidation. GLAD = glyceraldehyde, DHA = dihydroxyacetone, GA = glycolic acid, FA = formic acid.

System	Light employed	Main product (selectivity)	Productivity
TiO_2[5]	355 nm	FA (37%)	5.3 mmol $g_{PC}^{-1} \cdot h^{-1}$
$Na_4W_{10}O_{32}$[6]	>290 nm	GLAD (32.8%)	1075 μmol $g_{PC}^{-1} \cdot h^{-1}$ (5.25 TON) [a]
$Na_4W_{10}O_{32}/SiO_2$[6]	>290 nm	GLAD (59.4%)	119 μmol $g_{PC}^{-1} \cdot h^{-1}$ [b]
Anthraquinone disulfonate[2]	Blue LED 415 nm (200 $mW \cdot cm^{-2}$)	FA (77% among solution products)	4.1 mmol $g_{PC}^{-1} \cdot h^{-1}$
BiOBr (Bismuth oxybromide)[7]	UV: 120W UV high-pressure mercury lamp, 5.93 $mW \cdot cm^{-2}$	GA (50%)	5.3 mmol $g_{PC}^{-1} \cdot h^{-1}$ [c]
$ZnO/CuInS_2$[8]	White: xenon lamp (350 – 110 nm, 300 W)	DHA (41%)	333 μmol $g_{PC}^{-1} \cdot h^{-1}$ [d]
FTO|TiO_2|AP11 photoelectrode[9] AP11 = thienopyrroledione-based dye	White (100 $mW \cdot cm^{-2}$)	GLAD	3 $\mu molh^{-1}$ with a 0.64 cm^2 photoelectrode with an applied potential of 0.1 V vs Ag/AgCl
$AuPt/TiO_2$[10]	White(200 $mWcm^{-2}$)	GLA(60%)	1.69 mmol $g_{PC}^{-1} \cdot h^{-1}$
$ZnO/CuInS_2$[8]	300 W Xenon lamp (350 ~ 1100 nm)	DHA(41.1%)	27 μmol $g_{PC}^{-1} \cdot h^{-1}$
0.5% $Au@TiO_2$[11]	White(60 $mWcm^{-2}$)	GLAD(52%)	2.56 mmol $g_{PC}^{-1} \cdot h^{-1}$
1 %Cu/TiO_2[12]	White (100 $mWcm^{-2}$)	Glycolaldehyde, GCA (70 %)	1.902 mmol $g_{PC}^{-1} \cdot h^{-1}$
TiO_2 –CoNiP-5:5[13]	White (100 $mWcm^{-2}$)	GA(85%)	2.72 mmol $g_{PC}^{-1} \cdot h^{-1}$ [e]
$QA_{312}TiO_2$ (this work)	White (200 $mW \cdot cm^{-2}$)	GLAD (84%)	58 μmol $g_{PC}^{-1} \cdot h^{-1}$
$QA_{312}TiO_2$ (this work)	525 nm (120 $mW \cdot cm^{-2}$)	GLAD (76%)	38 μmol $g_{PC}^{-1} \cdot h^{-1}$
$QA_{312}TiO_2$ (this work)	590 nm (200 $mW \cdot cm^{-2}$)	GLAD (74%)	46 μmol $g_{PC}^{-1} \cdot h^{-1}$
$QA_{312}TiO_2$ (this work)	620 nm (33 $mW \cdot cm^{-2}$)	GLAD (80%)	47 μmol $g_{PC}^{-1} \cdot h^{-1}$ 20 TON based on QA

[a]6.3 μmol of GLAD with 400 μM $Na_4W_{10}O_{32}$, 3 mL, 2 hours of reaction. [b]5.7 μmol of GLAD with 8 $mgmL^{-1}$ $Na_4W_{10}O_{32}/SiO_2$, 3 mL, 2 hours of reaction. [c]Glycerol conversion of 85% and a selectivity for GA of 50% after 8 h, in 100 mL of 0.3 M glycerol with 300 mg BiOBr photocatalyst. [d] calculated from a glycerol oxidation rate of 0.27 mM h^{-1} and a selectivity of 41% with 10 mg $ZnO/CuInS_2$ photocatalyst in 30 mL. [e] calculated from a glycerol oxidation rate of 80 mmol g^{-1} and a selectivity of 85% after 25h.

Table S3. Photochemical glycerol oxidation with nanoparticles employed in this work. The distribution of product refers to HPLC analysis after 20 h irradiation.

White light 200 mWcm^{-2}, different QA loading					
#	**Photocatalyst**	**GLAD / mM**	**DHA / mM**	**GA / mM**	**FA / mM**
1	TiO_2 2 mgmL^{-1}	0.476	0.141	0.031	0.094
2	QA_{16}@TiO_2, 2 mgmL^{-1}	0.955	0.291	0.092	0.378
3	QA_{78}@TiO_2, 2 mgmL^{-1}	1.000	0.442	0.053	0.271
4	QA_{156}@TiO_2, 2 mgmL^{-1}	1.883	0.272	0.107	0.112
5	QA_{312}@TiO_2, 2 mgmL^{-1}	2.335	0.208	0.075	0.158
6	QA_{624}@TiO_2, 2 mgmL^{-1}	1.860	0.241	0.080	0.182
White light 200 mWcm^{-2}, different NPs amount					
#	**Photocatalyst**	**GLAD / mM**	**DHA / mM**	**GA / mM**	**FA / mM**
7	QA_{312}@TiO_2, 1 mgmL^{-1}	1.256	0.312	0.611	0.312
8	QA_{312}@TiO_2, 4 mgmL^{-1}	1.750	0.252	0.223	0.143
White light 200 mWcm^{-2}, control tests					
#	**Photocatalyst**	**GLAD / mM**	**DHA / mM**	**GA / mM**	**FA / mM**
9	QA_{312}@TiO_2, 2 mgmL^{-1},No TEMPO	0.108	0.127	0.045	0.100
10	QA_{312}@TiO_2, 2 mgmL^{-1}, O_2	2.431	0.258	0.194	0.120
11[a]	QA_{312}@TiO_2, 2 mgmL^{-1}, N_2	0.933	0.141	0.122	0.222
[a]Besides the obvious abatement in the photochemical oxidation activity under nitrogen atmosphere, the residual reactivity may suggest the role of TEMPO as electron acceptor in the photochemical cycle.[14]					
Green (525 nm, 120 mWcm^{-2}) and Yellow (590 nm, 200 mWcm^{-2}) light					
#	**Photocatalyst**	**GLAD / mM**	**DHA / mM**	**GA / mM**	**FA / mM**
12	QA_{312}@TiO_2, 2 mgmL^{-1}	1.535	0.109	0.076	0.309
13	TiO_2 2 mgmL^{-1}	0.121	0.057	0.013	0.029
14	QA_{312}@TiO_2, 2 mgmL^{-1}	1.835	0.122	0.152	0.366
15	TiO_2 2 mgmL^{-1}	0.149	0.049	0.012	0.014

Table S3 (continues). Photochemical glycerol oxidation with nanoparticles employed in this work. The distribution of product refers to HPLC analysis after 20 h irradiation.

Red light (620 nm, 33 mWcm^{-2})					
#	**Photocatalyst**	**GLAD / mM**	**DHA / mM**	**GA / mM**	**FA / mM**
16[b]	QA_{312}@TiO_2, 2 mgmL^{-1}	0.88	0.17	0.06	0.34
17	QA_{312}@TiO_2, 2 mgmL^{-1}	1.9±0.2	0.15±0.05	0.10±0.05	0.23±0.10
18	TiO_2 2 mgmL^{-1}	0.07±0.01	0.02±0.01	0.01±0.01	0.01±0.01
19	$Indigo_{312}$@TiO_2 2 mgmL^{-1}	0.10±0.02	0.03±0.01	0.06±0.02	n.d.
20	$Cibalakrot_{312}$@TiO_2 2 mgmL^{-1}	0.39±0.02	0.09±0.01	0.02±0.01	n.d.
21	QA_{312}@TiO_2, recycle 1	2.44	0.21	0.12	0.28
22	QA_{312}@TiO_2, recycle 2	2.05	0.23	0.09	0.09
23	QA_{312}@TiO_2, recycle 3	1.82	0.15	0.16	0.04
24	QA_{312}@TiO_2, recycle 4	2.07	0.22	0.08	0.15
25	QA_{312}@TiO_2, recycle 5	2.09	0.20	0.06	0.14
[b] after 4 h irradiation					

References

1 A. E. B. S. Stone, A. Fortunato, X. Wang, E. Saggioro, R. Q. Snurr, J. T. Hupp, F. Arcudi and L. Dordevic, *Adv. Mater.*, 2024, article number: 2408658.

2 E. Tacchi, G. Rossi, M. Natali, L. Đorđević and A. Sartorel, *Adv. Sustain. Syst.*, 2024, 2400538.

3 P. D. Josephy, T. Eling and R. P. Mason, *J. Biol. Chem.*, 1982, **257**, 3669–3675.

4 E. F. Paulus, F. J. J. Leusen and M. U. Schmidt, *CrystEngComm*, 2007, **9**, 131–143.

5 M. Liu, H. Liu, N. Li, C. Zhang, J. Zhang and F. Wang, *ChemSusChem*, 2022, **15**, e202201068.

6 A. Molinari, A. Maldotti, A. Bratovcic and G. Magnacca, *Catal. Today*, 2013, **206**, 46–52.

7 P. Limpachanangkul, P. Nimmmanterdwong, L. Liu, M. Hunsom, K. Pruksathorn, P. Piumsomboon and B. Chalermsinsuwan, *Sci. Rep.*, 2023, **13**, 1–8.

8 K. Meng, J. Zhang, B. Cheng, X. Ren, Z. Xia and F. Xu, *Adv. Mater.*, 2024, **36**, 2406460.

9 D. F. Bruggeman, A. Laoprte, R. J. Detz, S. Mathew and J. N. H. Reek, *Angew. Chem. Int. Ed.*, 2022, **61**, e202200175.

10 X. Liu, Y. Zou and J. Jiang, *Appl. Catal. B Environ. Energy*, 2024, **350**, 123927.

11 H. Bajpai, I. Chauhan, K. N. Salgaonkar, N. B. Mhamane and C. Gopinath, *RSC Sustain.*, 2023, **1**, 481–493.

12 H. Bajpai, T. R. Nivedhitha, E. Dais, S. S. Kanungo and C. S. Gopinath, *J. Catal.*, 2024, **437**, 115644.

13 T. R. Nivedhitha, H. Bajpai, J. V. Oommen, A. Abraham, I. Chauhan and C. S. Gopinath, *ACS Sustain. Chem. Eng.*, 2024, **12**, 14841–14853.

14 X. Zhao, J. Yang and J. Cheng, *J. Org. Chem.*, 2023, **88**, 540–547.